MEDICAL SCIENCE MONITOR

ANIMAL STUDY

e-ISSN 1643-3750
© Med Sci Monit, 2018; 24: 7914-7928
DOI: 10.12659/MSM.907412

Received: 2017.10.05
Accepted: 2018.03.05
Published: 2018.11.05

Tangshen Formula Treatment for Diabetic Kidney Disease by Inhibiting Racgap1-stata5-Mediated Cell Proliferation and Restoring miR-669j-Arntl-Related Circadian Rhythm

Authors' Contribution:
Study Design A
Data Collection B
Statistical Analysis C
Data Interpretation D
Manuscript Preparation E
Literature Search F
Funds Collection G

ADEF 1 **Xiuying Wang**
BF 2 **Hai Zhao**
BDF 3 **Xingquan Wu**
BCD 1 **Guangsheng Xi**
ADE 1 **Shengxue Zhou**

1 College of Chinese Medicine, Jilin Agricultural Science and Technology College, Jilin City, Jilin, P.R. China
2 Department of Reconstructive and Plastic Surgery, The General Hospital of Shenyang Military, Shenyang, Liaoning, P.R. China
3 Zang-fu Massage, Affiliated Hospital of Changchun University of Chinese Medicine, Changchun, Jilin, P.R. China

Corresponding Author: Shengxue Zhou, e-mail: zhoushengxue1111@163.com
Source of support: This study was supported by the Chinese Medicine Key Advantages Program of the Provincial Subjects of Jilin Agricultural Science and Technology College in Jilin province

Background: The aim of this study was to investigate the underlying mechanisms of Tangshen formula (TSF) for treatment of diabetic kidney disease (DKD).

Material/Methods: Microarray dataset GSE90842 was collected from the Gene Expression Omnibus database, including renal cortical tissues from normal control (NC), DKD, and DKD mice given TSF for 12 weeks (TSF) (n=3). Differentially-expressed genes (DEGs) were identified using LIMMA method. A protein-protein interaction (PPI) network was constructed using data from the STRING database followed by module analysis. The Mirwalk2 database was used to predict the underlying miRNAs of DEGs. Function enrichment analysis was performed using the DAVID tool.

Results: A total of 2277 and 2182 genes were identified as DEGs between DKD and NC or TSF groups, respectively. After overlap, 373 DEGs were considered as common in 2 comparison groups. Function enrichment indicated common DEGs were related to cell proliferation (Asf1b, anti-silencing function 1B histone chaperone; Anln, anillin, actin-binding protein; Racgap1, Rac GTPase activating protein 1; and Stat5, signal transducer and activator of transcription 5) and circadian rhythm (Arntl, aryl hydrocarbon receptor nuclear translocator-like). Racgap1 was considered as a hub gene in the PPI network because it could interact with Asf1b, Anln, and Stat5. Arntl was regulated by miR-669j in the miRNA-DEGs network and this miRNA was also a DEG in 2 comparisons.

Conclusions: TSF may be effective for DKD by inhibiting Racgap1-stata5-mediated cell proliferation and restoring miR-669j-Arntl-related circadian rhythm.

MeSH Keywords: **Cell Proliferation • Circadian Rhythm • Diabetic Nephropathies • MicroRNAs**

Full-text PDF: https://www.medscimonit.com/abstract/index/idArt/907412

2983 5 5 47

This work is licensed under Creative Common Attribution-NonCommercial-NoDerivatives 4.0 International (CC BY-NC-ND 4.0)

Indexed in: [Current Contents/Clinical Medicine] [SCI Expanded] [ISI Alerting System] [ISI Journals Master List] [Index Medicus/MEDLINE] [EMBASE/Excerpta Medica] [Chemical Abstracts/CAS]

Background

Diabetes is the third most common chronic disease worldwide (after cancer and cardiovascular diseases) and is associated with economic development. According to the International Diabetes Federation, 366 million people had diabetes in 2011 and this will reach 552 million by year 2030 [1]. China is one of the countries with the largest numbers of people with diabetes (90.0 million in 2011 and 129.7 million by 2030) [1]. Diabetic kidney disease (DKD) is the most prevalent and serious microvascular complication following diabetes. It is estimated that DKD is developed concomitantly in more than 60% of persons with diabetes [2]. Persistent albuminuria/proteinuria excretion indicates kidney function is damaged. DKD is difficult to reverse and easily progresses to chronic renal failure and end-stage renal disease, ultimately resulting in disability or death [3]. Thus, diabetes-associated DKD has become a significant public health problem that needs to be addressed.

Currently, DKD can be managed by glycemic control, antihypertensive drugs (angiotensin-converting enzyme, angiotensin receptor blocker, and calcium channel blocker) and antilipemic agents [4–6]. Although all these treatments seem to be effective, adverse reactions (e.g., hypotension, hyperkalemia, renal, urinary and respiratory disorders) after long-term use have been well documented [7,8]. Thus, investigation of more effective and safe treatment strategies is a clinically important issue.

Compared with target-oriented Western medicine, Traditional Chinese Medicine (TCM) maintains the body's normal function or homeostasis based on a holistic and synergistic theory to restore the balance of Yin-Yang of body energy [9]. In addition, TCM uses a combination of plants, minerals, and animal parts for treatment of diseases, several of which are medicinal and edible, inducing few adverse effects [10]. Therefore, TCM treatment is suggested as an effective and safe alternative for treatment of DKD [10,11]. Tangshen formula (TSF) is a commonly prescribed Chinese herbal medicine for diabetic renal injuries. A recent prospective, multicenter, double-blind, randomized, controlled study has demonstrated the significant benefit of TSF in decreasing proteinuria and improving estimated glomerular filtration rate in DKD patients compared with placebo [12]. Further studies indicate TSF may attenuate DKD by inhibiting zinc finger and BTB domain containing 16 (ZBTB16/PLZF) expression [13], transforming growth factor beta (TGF-β)/SMAD family member 3 (Smad3)/nuclear factor kappa B subunit (NF-κB) signaling pathways [14], and activating Janus kinase (JAK)/signal transducer and activator of transcription (STAT)/suppressor of cytokine signaling (SOCS) signaling pathway [15]. However, the mechanism of TSF in DKD treatment remains unclear.

The goal of this study was to further explore the molecular mechanisms of TSF treatment for DKD by collecting microarray dataset GSE90842 from the National Center of Biotechnology Information Gene Expression Omnibus (NCBI GEO) public database [13] and analyzing it by a series of bioinformatics software. Compared with the study of Zhao et al. [13], a non-strict threshold (P<0.05 and |logFC (fold change) | >0.1 *vs.* |logFC| >0.5) was selected to obtain more differentially-expressed genes (DEGs), and DEGs were run between the 2 groups by *t* test but not among the 3 groups by one-way ANOVA. The crucial DEGs were subsequently identified by construction of a protein and protein interaction (PPI) network and module analysis. The underlying microRNAs (miRNAs) regulating DEGs and the small molecular drugs having similar functions to TSF were also predicted. These studies were not performed by Zhao et al. [13]. Our findings may provide new insights into the mechanisms of TSF treatment for DKD.

Material and Methods

Microarray data

Microarray dataset GSE90842 was downloaded from NCBI GEO (*http://www.ncbi.nlm.nih.gov/geo/*), which included renal cortical tissue samples from 20-week-old male C57BLKS/J db/m mice (normal control group, NC, n=3), 20-week-old male C57BLKS/J db/db mice (DKD group, n=3), and db/db mice given TSF by intra-gastric gavage (2.4 g/kg/day) for 12 weeks (TSF group, n=3). The non-treatment mice were administered saline. Experiments were approved by the Ethics Committee of the China-Japan Friendship Institute of Clinical Medical Sciences and performed in accordance with the NIH Guiding Principles for the Care and Use of Laboratory Animals [13].

Data normalization and DEGs identification

The raw CEL files were preprocessed and normalized using the Robust Multichip Average (RMA) algorithm [16] in the R Bioconductor affy package (*http://www.bioconductor.org/packages/release/bioc/html/affy.html*). The DEGs between DKD and NC/TSF group were screened using the Linear Models for Microarray data (LIMMA) method [17] in the Bioconductor R package (*http://www.bioconductor.org/packages/release/bioc/html/limma.html*). The cutoff point of P<0.05 and |logFC| >0.1 were set to obtain more DEGs. A heatmap of DEGs was constructed using R package pheatmap (*http://cran.r-project.org/web/packages/pheatmap/index.html*). A Venn diagram was constructed to screen the DEGs between DKD and NC groups that were reversed by TSF treatment using an online tool (*http://bioinformatics.psb.ugent.be/webtools/Venn/*).

This work is licensed under Creative Common Attribution-NonCommercial-NoDerivatives 4.0 International (CC BY-NC-ND 4.0)

Indexed in: [Current Contents/Clinical Medicine] [SCI Expanded] [ISI Alerting System] [ISI Journals Master List] [Index Medicus/MEDLINE] [EMBASE/Excerpta Medica] [Chemical Abstracts/CAS]

PPI network construction

The DEGs were mapped into the PPI data retrieved from the STRING 10.0 (Search Tool for the Retrieval of Interacting Genes; *http://string db.org/*) database [18] to construct the PPI network, with the threshold value set as the combined scores >0.9. The PPI network was visualized using Cytoscape software 2.8 (*www.cytoscape.org/*) [19]. The hub genes with more interactions with other genes (degree) were selected and plotted with ggplot2 in R package (*http://www.R-project.org/*). To identify functionally related and highly interconnected clusters from the PPI network, module analysis was then conducted using the Molecular Complex Detection (MCODE) plugin of Cytoscape software. The parameters were set as: degree cutoff=6, node score cutoff=0.2, k-core=5, and maximum depth=100 (*ftp://ftp.mshri.on.ca/pub/BIND/Tools/MCODE*) [20]. Modules with MCODE score ≥4 and nodes ≥6 were considered significant.

miRNA prediction

The DEGs-related miRNAs were predicted using the Mirwalk2 database (*http://www.zmf.umm.uni-heidelberg.de/apps/zmf/mirwalk2*) [21], which provides the largest collection of predicted and experimentally verified miR-target interactions with various miRNA databases. Then, the miRNA-target gene interaction network was constructed and visualized using Cytoscape software 2.8 (*www.cytoscape.org/*) [19].

Function enrichment analysis

Kyoto encyclopedia of genes and genomes (KEGG) pathway and Gene ontology (GO) enrichment analyses were carried out to explore the underlying functions of all DEGs and genes in PPI network and modules using the Database for Annotation, Visualization and Integrated Discovery (DAVID) 6.8 online tool (*http://david.abcc.ncifcrf.gov*). P<0.05 was set as the threshold to screen the significant GO biological process (BP) terms and KEGG.

Screening of small-molecule drugs similar to TSF treatment

The Connectivity Map (CMAP, *http://www.broadinstitute.org/cmap/*), which contains more than 7000 expression signatures involving 6100 small molecules as treatment-control pairs, was used to compare the DEGs with genes perturbed by small molecules in the CMAP database, to identify underlying drugs associated with these DEGs. A correlation score for each corresponding small molecule was calculated, ranging from –1 to 1. A high positive connectivity score (close to +1) indicates that the corresponding small molecule induced the expression of the query signature, while a high negative connectivity score (close to –1) indicates that the corresponding small molecule reversed the expression of the query signature. Significant small-molecule drugs were selected according to the threshold value of p<0.05 and |mean| >0.4.

Results

Identification of DEGs

According to the threshold of p<0.05 and |logFC| >0.1, there were 2277 genes identified as DEGs between NC and DKD groups, including 1138 upregulated and 1139 downregulated genes, while 2182 genes were identified as DEGs between TSF and DKD groups, including 1152 upregulated and 1130 downregulated genes. The clustering analysis in heatmap indicated that the identified DEGs perform well in distinguishing between the 2 groups (Figure 1).

Further, a Venn diagram was used to obtain the overlap of the upregulated (downregulated) DEGs between NC and DKD with the downregulated (upregulated) DEGs between TSF and DKD (i.e., the DEGs changed in DKD can be reversed by TSF). As a result, 193 common DEGs (including 4 miRNAs) were identified between the upregulated DEGs of NC and DKD comparison and the downregulated DEGs of TSF and DKD comparison (defined as downregulated), while 180 common DEGs (including 14 miRNAs) were identified between downregulated DEGs of NC and DKD comparison and the upregulated DEGs of TSF and DKD comparison (defined as upregulated) (Figure 2, Table 1).

Function enrichment analysis for common DEGs

The potential functions of all common DEGs were predicted by the online tool DAVID. As a result, 12 GO BP terms and 7 KEGG pathways were enriched for DEGs. The GO BP terms mainly included transcription, DNA-templated (anti-silencing function 1B histone chaperone, Asf1b: logFC=0.62, p-value=6.71E-03, NC *vs.* DKD; logFC=–0.38, p-value=5.93E-03, TSF *vs.* DKD), positive regulation of cell proliferation (Stat5a: logFC=–0.39, p-value=3.35E-03, NC *vs.* DKD; logFC=0.27, p-value 5.43E-03, TSF *vs.* DKD) and cell division (anillin, actin-binding protein, Anln: logFC=0.80, p-value=4.76E-03, NC *vs.* DKD; logFC=–0.46, p-value=3.85E-02, TSF *vs.* DKD; Rac GTPase activating protein 1, Racgap1: logFC=0.44, p-value=1.81E-03, NC *vs.* DKD; logFC=–0.18, p-value=2.80E-02, TSF *vs.* DKD; cell division cycle 25B, Cdc25b: logFC=0.23, p-value=4.98E-02, NC *vs.* DKD; logFC=–0.30, p-value=1.80E-02, TSF *vs.* DKD), while the enriched KEGG pathways were nerve conduction-related, including neuroactive ligand-receptor interaction and cholinergic synapse (cholinergic receptor muscarinic 1, Chrm1: logFC=–0.23, p-value=2.368E-02, NC *vs.* DKD; logFC=0.18, p-value=2.72E-02, TSF *vs.* DKD) (Table 2).

This work is licensed under Creative Common Attribution-NonCommercial-NoDerivatives 4.0 International (CC BY-NC-ND 4.0)

Indexed in: [Current Contents/Clinical Medicine] [SCI Expanded] [ISI Alerting System] [ISI Journals Master List] [Index Medicus/MEDLINE] [EMBASE/Excerpta Medica] [Chemical Abstracts/CAS]

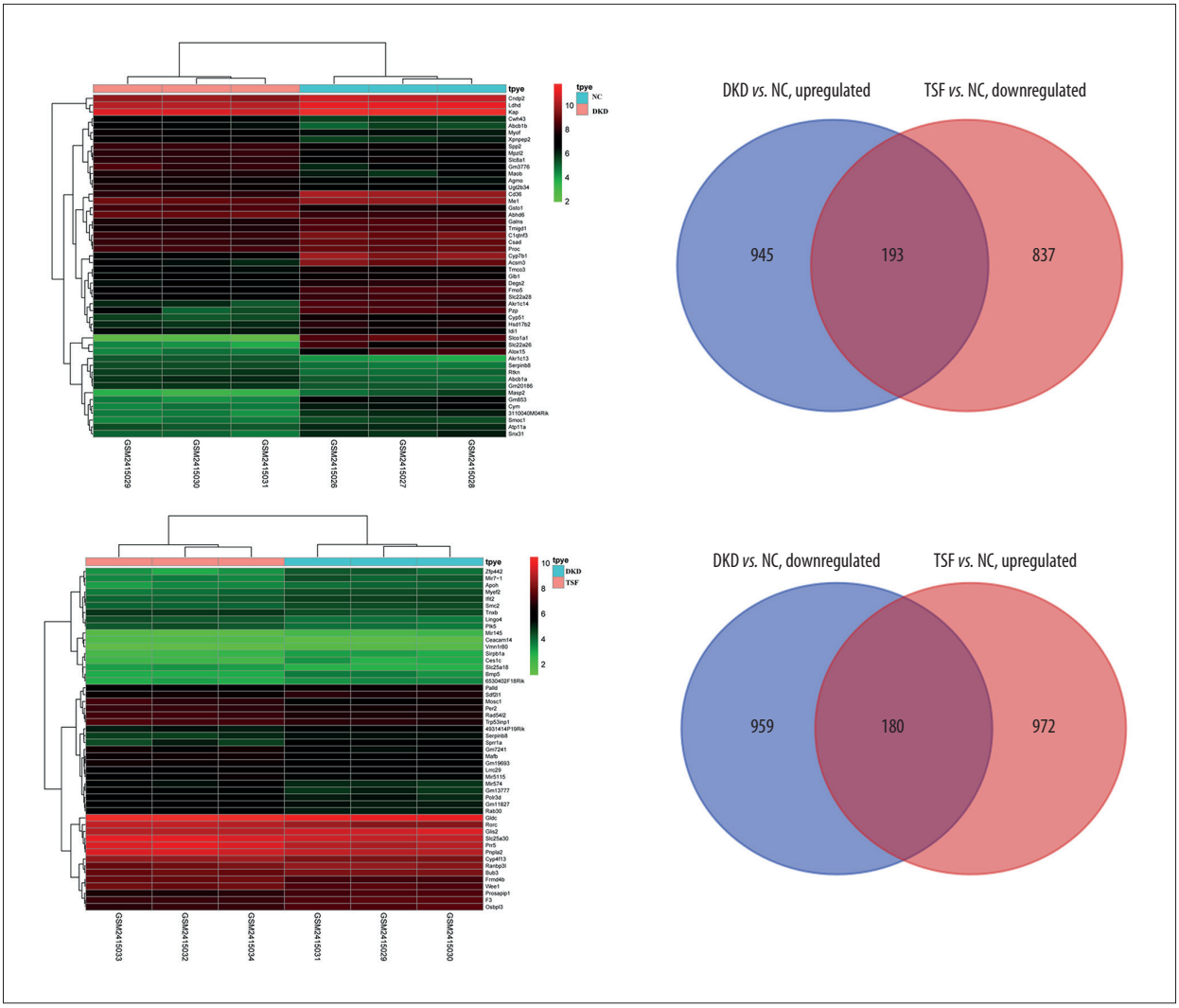

Figure 1. Differentially-expressed genes between DKD and NC/TSF. A, heat map of top 50 differentially-expressed genes between DKD and NC; B, heat map of top 50 differentially-expressed genes between DKD and TSF; C, Venn diagram to obtain the overlap of the upregulated (downregulated) DEGs between NC and DKD with the downregulated (upregulated) DEGs between TSF and DKD. NC – normal control; DKD – diabetic kidney disease; TSF – Tangshen formula. High-level expression is indicated by red and low-level expression is indicated by green.

PPI network construction and modules analysis for DEGs

A PPI network was constructed to screen crucial genes associated with TSF treatment, including 106 nodes (59 upregulated and 47 downregulated) and 143 edges (interaction relationships) (Figure 3). After calculating the degree, Racgap1 (degree=12), Asf1b (degree=9) and Anln (degree=6) were found to be hub genes (Figure 3). In addition to regulation of cell proliferation, cell cycle, and nerve conduction, the DEGs in PPI were also involved in circadian rhythm (aryl hydrocarbon receptor nuclear translocator-like, Arntl: logFC=–1.01, p-value=3.81E-02, NC *vs.* DKD; logFC=0.62, p-value=3.96E-02, TSF *vs.* DKD) (Table 3). Further, 1 significant module was screened from the PPI network (Figure 4), which was also enriched into cell division- and cell cycle-related GO terms (without no pathways enriched), demonstrating these processes may be especially important mechanisms for TSF treatment (Table 4).

DEGs-related miRNAs

After searching the Mirwalk2 database, 145 miRNAs were found to regulate the above common DEGs, which was used to construct a miRNA-DEGs network, including 181 interaction pairs and 24 DEGs. As shown in Figure 5, Asf1b and Anln were regulated by mmu-miR-703, which was significantly upregulated in DKD compared with NC (logFC=0.59, p-value=1.46E-02); Arntl was regulated by mmu-miR-669j, which was a DEG in

This work is licensed under Creative Common Attribution-NonCommercial-NoDerivatives 4.0 International (CC BY-NC-ND 4.0)

Indexed in: [Current Contents/Clinical Medicine] [SCI Expanded] [ISI Alerting System] [ISI Journals Master List] [Index Medicus/MEDLINE] [EMBASE/Excerpta Medica] [Chemical Abstracts/CAS]

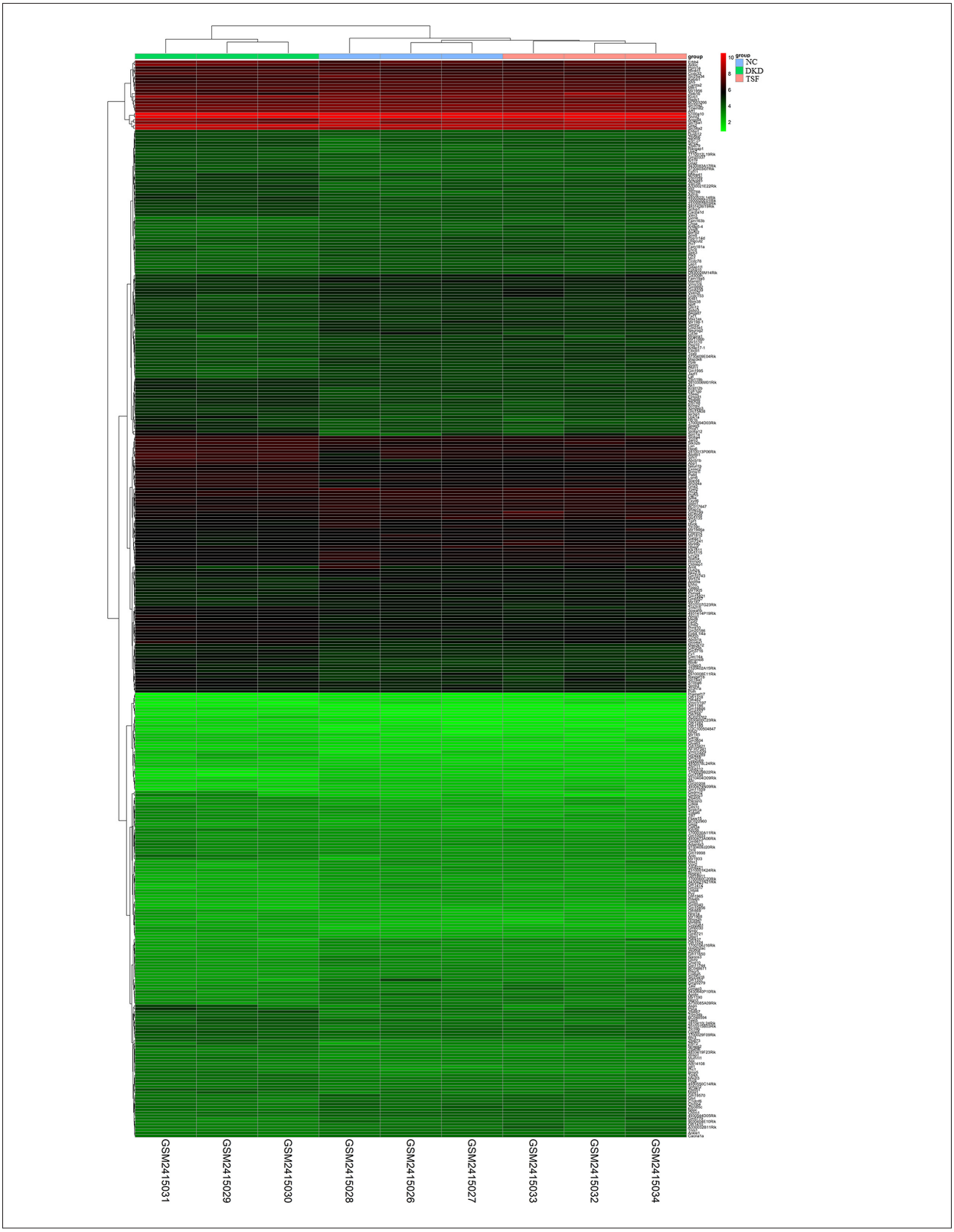

Figure 2. Heat map showing all common differentially-expressed genes between DKD *vs.* NC and DKD *vs.* TSF. NC – normal control; DKD – diabetic kidney disease; TSF – Tangshen formula. High-level expression is indicated by red and low-level expression is indicated by green.

This work is licensed under Creative Common Attribution-NonCommercial-NoDerivatives 4.0 International (CC BY-NC-ND 4.0)

Indexed in: [Current Contents/Clinical Medicine] [SCI Expanded] [ISI Alerting System] [ISI Journals Master List] [Index Medicus/MEDLINE] [EMBASE/Excerpta Medica] [Chemical Abstracts/CAS]

Table 1. Top 20 differentially expressed genes common between two comparisons.

Gene	DKD *vs.* NC		TSF *vs.* DKD	
	LogFC	P-value	LogFC	P-value
Mir145	0.67	5.13E-03	–0.72	6.61E-05
Palld	0.24	1.67E-02	–0.53	2.48E-04
Serpinb8	0.69	3.11E-05	–0.62	2.49E-04
Sirpb1a	0.45	1.84E-05	–0.65	4.66E-04
Bmp5	0.46	3.83E-03	–0.61	5.2E-04
Sprr1a	1.66	3.73E-04	–1.01	5.41E-04
Ces1c	0.39	3.92E-02	–0.70	6.22E-04
Ifit2	0.47	2.67E-02	–0.41	8.46E-04
Glis2	0.21	4.92E-02	–0.41	8.46E-04
Smc2	0.53	2.70E-03	–0.31	9.46E-04
4931414P19Rik	0.33	6.16E-03	–0.40	9.71E-04
Rtn4r	0.50	9.87E-04	–0.41	1.27E-03
Prc1	0.60	4.03E-03	–0.44	1.33E-03
Stard4	0.59	1.61E-02	–0.38	1.34E-03
Dusp12	0.30	3.54E-03	–0.35	1.35E-03
2610008E11Rik	0.57	1.26E-02	–0.33	1.61E-03
Upk2	0.44	2.48E-02	–0.51	1.70E-03
Mir1933	0.57	1.29E-02	–0.53	1.85E-03
Tnfsf15	0.40	2.19E-02	–0.76	1.93E-03
Gm19846	0.37	4.17E-03	–0.36	2.05E-03
Cd3e	–0.85	3.58E-04	0.23	4.79E-02
Slc25a18	–0.39	1.10E-03	0.43	5.75E-04
Gzmk	–0.55	1.12E-03	0.29	2.49E-02
Ston1	–0.37	1.22E-03	0.26	3.80E-02
Mir1905	–0.53	1.35E-03	0.21	4.86E-02
Plk5	–0.48	1.52E-03	0.44	9.33E-04
Gm20208	–0.35	1.53E-03	0.23	6.76E-03
Olfr1272	–0.59	1.57E-03	0.30	6.77E-03
A730085A09Rik	–0.49	1.81E-03	0.29	2.50E-02
Il28a	–0.45	1.84E-03	0.48	1.57E-03
Enho	–0.36	2.09E-03	0.35	5.48E-03
Pde6h	–0.37	2.25E-03	0.36	9.10E-03
Gm7241	–0.47	2.48E-03	0.85	7.62E-04
Neurog2	–0.60	2.67E-03	0.27	3.79E-02
Mir1956	–0.52	2.68E-03	0.60	1.34E-03
Gm12	–0.32	2.69E-03	0.30	4.85E-03
Msx1	–0.45	2.69E-03	0.29	7.65E-03
Mamld1	–0.60	3.10E-03	0.47	7.45E-03
Plscr5	–0.30	3.22E-03	0.19	0.20E-02
Ghrhr	–0.42	3.64E-04	0.33	2.51E-03

NC – normal control; DKD – diabetic kidney disease; TSF – Tangshen formula; FC – fold change.

This work is licensed under Creative Common Attribution-NonCommercial-NoDerivatives 4.0 International (CC BY-NC-ND 4.0)

Indexed in: [Current Contents/Clinical Medicine] [SCI Expanded] [ISI Alerting System] [ISI Journals Master List] [Index Medicus/MEDLINE] [EMBASE/Excerpta Medica] [Chemical Abstracts/CAS]

Table 2. Significantly enriched functions for all differentially expressed genes.

Term	P-value	Genes
GO: 0006355~regulation of transcription, DNA-templated	3.95E-06	STAT5A, PHF20, ZFP788, ZFP873, ZFP879, ASF1B, NEUROG2, ABCG1, PPIE, MAMLD1...
GO: 0006357~regulation of transcription from RNA polymerase II promoter	4.25E-03	CAMTA2, STAT5A, GLIS2, BARHL2, TCEAL6, MYBL1, HES6, MED4, MAMLD1, TCEA2...
GO: 0060124~positive regulation of growth hormone secretion	6.50E-03	GABBR1, GHRL, GHRHR
GO: 0045165~cell fate commitment	1.24E-02	ERBB4, ONECUT2, BARHL2, NEUROG2, SOX8
GO: 0008284~positive regulation of cell proliferation	1.84E-02	SSBP3, SHMT2, ERBB4, PRC1, STAT5A, CAMP, BTC, EFNB2, PROX1, GHRHR...
GO: 0030512~negative regulation of transforming growth factor beta receptor signaling pathway	2.96E-02	ASPN, PEG10, ONECUT2, PPM1A
GO: 0055005~ventricular cardiac myofibril assembly	3.69E-02	NKX2-5, PROX1
GO: 0006351~transcription, DNA-templated	4.31E-02	STAT5A, ONECUT2, PHF20, MYBL1, SOX8, TAL2, ZFP879, HNRNPD, TCEA2, ASF1B...
GO: 0051301~cell division	4.51E-02	KIFC5B, PLK5, PRC1, NCAPG2, SPAG5, KATNB1, ANLN, RACGAP1, SMC2, CDC25B
GO: 0060024~rhythmic synaptic transmission	4.89E-02	NLGN3, CACNA1A
GO: 0000255~allantoin metabolic process	4.89E-02	STAT5A, ALLC
mmu04024: cAMP signaling pathway	4.47 E-03	HTR1B, VAV3, CHRM1, GABBR1, GHRL, GRIA3, VIPR2, CACNA1D
mmu04080: Neuroactive ligand-receptor interaction	9.74E-03	HTR1B, SSTR3, CHRM1, GABBR1, CHRNB4, GRIA3, NMBR, VIPR2, GHRHR
mmu04727: GABAergic synapse	1.30E-02	SLC38A2, GABBR1, GNB3, CACNA1D, CACNA1A
mmu04725: Cholinergic synapse	3.06E-02	CHRM1, CHRNB4, GNB3, CACNA1D, CACNA1A
mmu04724: Glutamatergic synapse	3.23E-02	SLC38A2, GRIA3, GNB3, CACNA1D, CACNA1A
mmu04010: MAPK signaling pathway	4.92E-02	MAP3K6, FGF11, PPM1A, CACNA1D, MAP3K12, CACNA1A, CDC25B
mmu04726: Serotonergic synapse	4.96E-02	HTR1B, SLC6A4, GNB3, CACNA1D, CACNA1A

The genes were enriched into Gene ontology (GO) biological process terms and Kyoto encyclopedia of genes and genomes (KEGG) pathways. The genes were differentially expressed between NC and DKD, and significantly reversed by TSF treatment. NC – normal control; DKD – diabetic kidney disease; TSF – Tangshen formula.

2 comparisons (logFC=0.35, p-value=1.13E-02, NC *vs.* DKD; logFC=–0.40, p-value=1.11E-02, TSF *vs.* DKD).

Small-molecule drugs similar to TSF treatment

The DEGs, including 180 upregulated and 193 downregulated DEGs, were analyzed by use of the CMAP tool. As a result, 37 small-molecule chemicals with positive mean and enrichment scores were predicted, including thioguanosine, withaferin-A, DL-thiorphan, and menadione, which indicated their potential similarity to TSF for treatment of DKD, and these may exert a synergistic effect (Table 5).

Discussion

Compared the study of Zhao et al. [13], more DEGs were screened between NC *vs.* DKD (2277 *vs.* 83) and TSF *vs.* DKD (2182 *vs.* 13) using the non-strict threshold in our present study, which led to more overlap among 2 comparisons (373 *vs.* 3, Pgm5, Zbtb16/PLZF, and Abcb1b). Although Pgm5 (phosphoglucomutase 5), Zbtb16/PLZF, and Abcb1b [ATP-binding cassette, subfamily B (MDR/TAP), member 1B] identified by Zhao et al. [13] were also found in our study, subsequent PPI network and topological property analysis excluded their importance (Pgm5, degree=1; Zbtb16/PLZF, degree=0; Abcb1b, degree=3). On the

This work is licensed under Creative Common Attribution-NonCommercial-NoDerivatives 4.0 International (CC BY-NC-ND 4.0)

Indexed in: [Current Contents/Clinical Medicine] [SCI Expanded] [ISI Alerting System] [ISI Journals Master List] [Index Medicus/MEDLINE] [EMBASE/Excerpta Medica] [Chemical Abstracts/CAS]

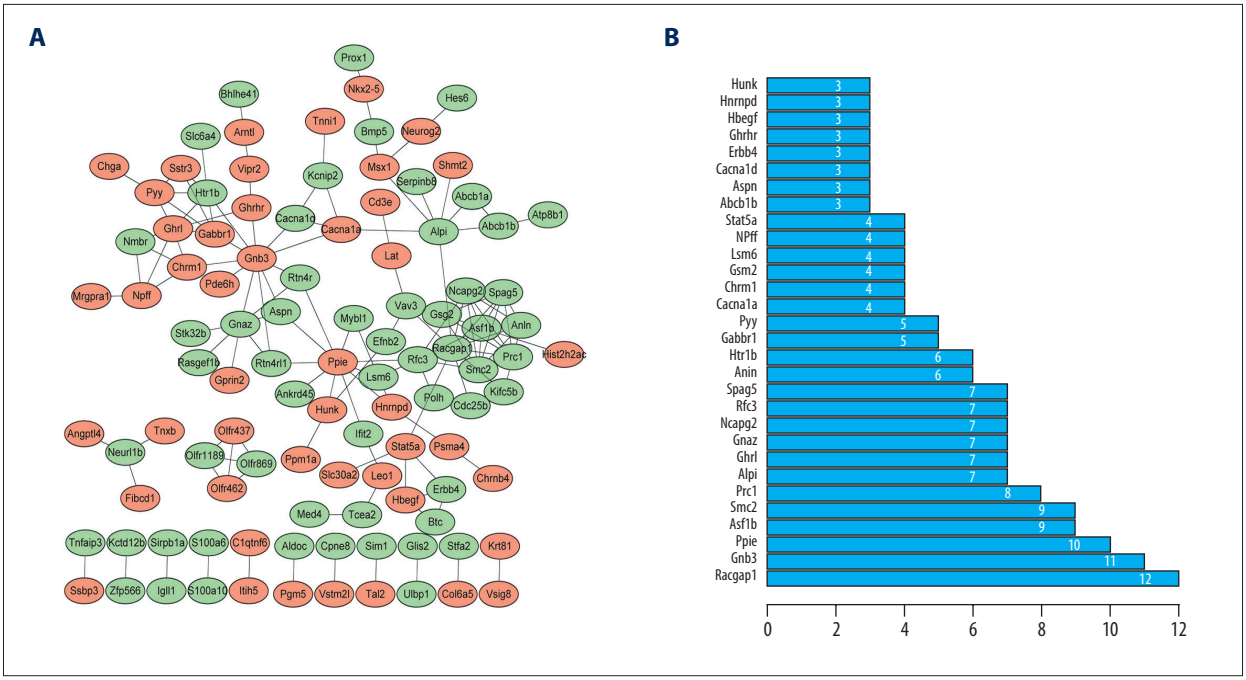

Figure 3. Protein-protein interaction network to screen crucial genes. (**A**) Protein-protein interaction network of differentially-expressed genes of overlap between DKD and NC/TSF. Upregulated genes are indicated by orange and downregulated genes are indicated by green. (**B**) Protein rank according their interaction pairs in the protein-protein interaction network.

Table 3. Significantly enriched functions for differentially expressed genes of PPI network.

Term	P-value	Genes
GO: 0008284~positive regulation of cell proliferation	7.10E-04	SSBP3, SHMT2, PRC1, ERBB4, STAT5A, BTC, EFNB2, HBEGF, NKX2-5, PROX1, GHRHR
GO: 0060124~positive regulation of growth hormone secretion	1.27E-03	GABBR1, GHRL, GHRHR
GO: 0051301~cell division	4.23E-03	KIFC5B, PRC1, NCAPG2, SPAG5, ANLN, RACGAP1, SMC2, CDC25B
GO: 0006357~regulation of transcription from RNA polymerase II promoter	5.83E-03	MED4, GLIS2, STAT5A, MYBL1, HES6, TCEA2, NKX2-5, SIM1
GO: 0007165~signal transduction	7.61E-03	GNAZ, STAT5A, GABBR1, RACGAP1, VIPR2, GHRHR, HTR1B, SSTR3, CHRM1, GNB3...
GO: 0007188~adenylate cyclase-modulating G-protein coupled receptor signaling pathway	1.46E-02	GNAZ, CACNA1D, GHRHR
GO: 0055005~ventricular cardiac myofibril assembly	1.62E-02	NKX2-5, PROX1
GO: 0045944~positive regulation of transcription from RNA polymerase II promoter	1.87E-02	SSBP3, MSX1, GLIS2, STAT5A, LEO1, NEUROG2, MYBL1, TCEA2, ARNTL, NKX2-5, PROX1, BMP5
GO: 0006355~regulation of transcription, DNA-templated	1.92E-02	STAT5A, GLIS2, NEUROG2, MYBL1, ARNTL, HES6, PROX1, TAL2, PPIE, ASF1B...
GO: 0007623~circadian rhythm	2.09E-02	SLC6A4, ARNTL, BHLHE41, PROX1
GO: 0035556~intracellular signal transduction	2.16E-02	SIRPB1A, HUNK, LAT, STK32B, VAV3, RACGAP1, GSG2
GO: 0046426~negative regulation of JAK-STAT cascade	2.27E-02	ASPN, RTN4RL1, RTN4R

This work is licensed under Creative Common Attribution-NonCommercial-NoDerivatives 4.0 International (CC BY-NC-ND 4.0)

Indexed in: [Current Contents/Clinical Medicine] [SCI Expanded] [ISI Alerting System] [ISI Journals Master List] [Index Medicus/MEDLINE] [EMBASE/Excerpta Medica] [Chemical Abstracts/CAS]

Table 3 continued. Significantly enriched functions for differentially expressed genes of PPI network.

Term	P-value	Genes
GO: 0006351~transcription, DNA-templated	2.43E-02	STAT5A, GLIS2, NEUROG2, MYBL1, ARNTL, HES6, PROX1, TAL2, MED4, ASF1B...
GO: 0007193~adenylate cyclase-inhibiting G-protein coupled receptor signaling pathway	2.47E-02	GNAZ, HTR1B, GABBR1
GO: 0007595~lactation	2.58E-02	ERBB4, STAT5A, GHRHR
GO: 0048511~rhythmic process	3.24E-02	HNRNPD, ARNTL, BHLHE41, PROX1
GO: 0045893~positive regulation of transcription, DNA-templated	3.70E-02	SSBP3, MED4, ERBB4, GLIS2, PPM1A, ARNTL, NKX2-5, PROX1
GO: 0051988~regulation of attachment of spindle microtubules to kinetochore	3.73E-02	SPAG5, RACGAP1
GO: 0002591~positive regulation of antigen processing and presentation of peptide antigen via MHC class I	3.73E-02	ABCB1A, ABCB1B
GO: 0002489~antigen processing and presentation of endogenous peptide antigen via MHC class Ib via ER pathway, TAP-dependent	0.042553	ABCB1A, ABCB1B
GO: 0019221~cytokine-mediated signaling pathway	4.50E-02	ASPN, RTN4RL1, STAT5A, RTN4R
GO: 0048845~venous blood vessel morphogenesis	4.77E-02	EFNB2, PROX1
GO: 0046010~positive regulation of circadian sleep/ wake cycle, non-REM sleep	4.77E-02	GHRL, GHRHR
GO: 0002485~antigen processing and presentation of endogenous peptide antigen via MHC class I via ER pathway, TAP-dependent	4.77E-02	ABCB1A, ABCB1B
GO: 0002481~antigen processing and presentation of exogenous protein antigen via MHC class Ib, TAP-dependent	4.77E-02	ABCB1A, ABCB1B
GO: 0030816~positive regulation of cAMP metabolic process	4.77E-02	CHGA, GHRHR
GO: 0007049~cell cycle	4.92E-02	PRC1, NCAPG2, SPAG5, ANLN, RACGAP1, SMC2, GSG2, CDC25B
mmu04024: cAMP signaling pathway	1.60E-03	HTR1B, VAV3, CHRM1, GABBR1, GHRL, VIPR2, CACNA1D
mmu04080: Neuroactive ligand-receptor interaction	2.22E-03	HTR1B, SSTR3, CHRM1, GABBR1, CHRNB4, NMBR, VIPR2, GHRHR
mmu04725: Cholinergic synapse	5.972E-03	CHRM1, CHRNB4, GNB3, CACNA1D, CACNA1A
mmu04726: Serotonergic synapse	1.02E-02	HTR1B, SLC6A4, GNB3, CACNA1D, CACNA1A
mmu04012: ErbB signaling pathway	1.85E-02	ERBB4, STAT5A, BTC, HBEGF
mmu04727: GABAergic synapse	1.85E-02	GABBR1, GNB3, CACNA1D, CACNA1A

The genes were enriched into Gene ontology (GO) biological process terms and Kyoto encyclopedia of genes and genomes (KEGG) pathways. The genes were differentially expressed between NC and DKD, and significantly reversed by TSF treatment. NC – normal control; DKD – diabetic kidney disease; TSF – Tangshen formula.

This work is licensed under Creative Common Attribution-NonCommercial-NoDerivatives 4.0 International (CC BY-NC-ND 4.0)

Indexed in: [Current Contents/Clinical Medicine] [SCI Expanded] [ISI Alerting System] [ISI Journals Master List] [Index Medicus/MEDLINE] [EMBASE/Excerpta Medica] [Chemical Abstracts/CAS]

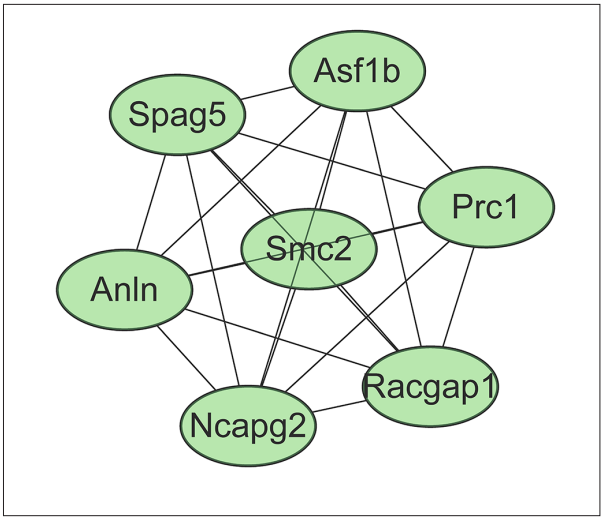

Figure 4. Significant modules screened from PPI network. Green indicates downregulated genes.

contrary, we preliminarily identified that Racgap1 (degree=12), Asf1b (degree=9), Anln (degree=6), and Stat5a (degree=4) were particularly important. Asf1b, Anln, and Racgap1 were significantly upregulated in DKD but were downregulated by TSF treatment, while the opposite result was observed for Stat5a, which was downregulated in DKD but upregulated after TSF treatment. These genes were enriched into cell growth (Asf1b, Anln, Racgap1, and Stat5). Arntl, which had a similar expression pattern to Stat5a, was considered to be pivotal because of its involvement in circadian rhythm, a specific pathway enriched by the genes in PPI. Accordingly, we believe TSF may be effective for treatment of DKD by the above pathways, which appears to be in line with previous studies directly or indirectly as shown by the following evidence.

It is widely accepted that glomerular mesangial expansion is one of the main pathologic characteristics of DKD, which develops due to mesangial cell proliferation and excessive accumulation of extracellular matrix (ECM) proteins [22–24]. Thus, suppressing cell growth to manage DKD has been extensively investigated in recent years [22–24]. In the present study we showed that TSF may also be effective for DKD by this mechanism because the related genes have been demonstrated to be associated with cell proliferation. It has been reported that depletion of histone H3–H4 chaperone Asf1b severely compromises proliferation, leading to aberrant nuclear structures and a distinct transcriptional signature, while its overexpression increases cellular proliferation, promoting tumor progression and predicting poor outcomes [25]. This effect of Asf1b was also observed in β cell proliferation [26]. Anln is an actin-binding protein required for cytokinesis. Similarly, several studies have proved Anln plays a critical role in human carcinogenesis and serves as a poor prognostic biomarker [27,28]. Knockdown of Anln by lentivirus results in G2/M phase arrest, cell growth, and migration inhibition, achieving the treatment goal for cancer [28,29]. Racgap1 is a component of the central spindle protein complex and is also essential for orchestrating cell division. Thus, its upregulated expression increases the potential of cell excessive proliferation and induces cancer [30]. However, there were no studies focusing on their roles (Cdc25b, Asf1b, Anln, and Racgap1) in DKD and they may be novel targets, which require further experiments to confirm.

Although the study of Hu et al. [15] has demonstrated TSF may be beneficial for DKD treatment via regulating the JAK/STAT/SOCS signaling pathway, only the expressions of Stat3 (upregulated) and Stat4 (downregulated) were detected. Stat5 was also upregulated after TSF in our study, indicating similar function to Stat3. Furthermore, a recent study indicates Racgap1 appears to be involved cytokinesis by translocation of Stat3. Both Racgap1 inhibitor and siRNA-mediated silencing treatment resulted in increased Stat3 phosphorylation and STAT3-driven transcriptional activity [31]. Thus, we speculated there was also an interaction between Racgap1 and Stat5, which was demonstrated in our PPI network. Also, Racgap1 was observed

Table 4. Significantly enriched functions for module genes screened from PPI network.

Term	Count	P-value	Genes
GO: 0051301~cell division	6	2.17E-08	PRC1, NCAPG2, SPAG5, ANLN, RACGAP1, SMC2
GO: 0007049~cell cycle	6	2.59E-07	PRC1, NCAPG2, SPAG5, ANLN, RACGAP1, SMC2
GO: 0007067~mitotic nuclear division	4	6.87E-05	NCAPG2, SPAG5, ANLN, SMC2
GO: 0051988~regulation of attachment of spindle microtubules to kinetochore	2	2.32E-03	SPAG5, RACGAP1
GO: 0030261~chromosome condensation	2	5.30E-03	NCAPG2, SMC2
GO: 0000281~mitotic cytokinesis	2	9.92 E-03	ANLN, RACGAP1

This work is licensed under Creative Common Attribution-NonCommercial-NoDerivatives 4.0 International (CC BY-NC-ND 4.0)

Indexed in: [Current Contents/Clinical Medicine] [SCI Expanded] [ISI Alerting System] [ISI Journals Master List] [Index Medicus/MEDLINE] [EMBASE/Excerpta Medica] [Chemical Abstracts/CAS]

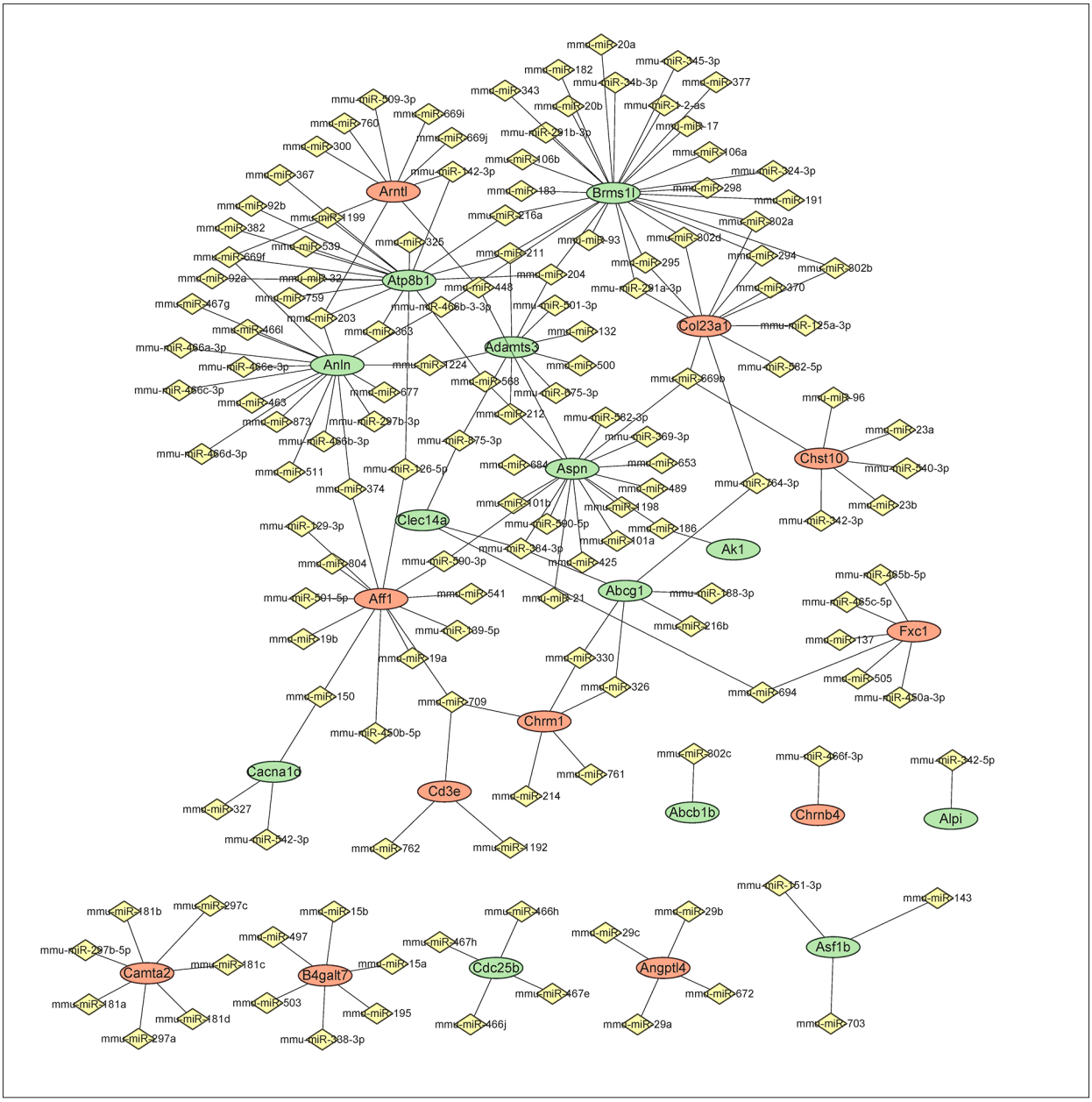

Figure 5. A miRNA-gene interaction network. Orange indicates upregulated genes and green indicates downregulated genes.

to interact with Anln and Asf1b. Therefore, Racgap1 may be an especially pivotal target in the treatment of TSF for DKD.

Normal circadian rhythms are crucial for maintaining physiological and functional homeostasis; once disrupted, pathological diseases may be triggered, such as diabetes [32]. Several studies have demonstrated the expression of clock (Per1, Period circadian clock 1; Per2; Arntl; CLOCK, circadian locomotor output cycles kaput; Cry1, cryptochrome 1), as well as clock-controlled genes (Dbp, D site albumin promoter binding protein; E4bp4, also known as NFIL3, nuclear factor, interleukin 3, regulated; RevErbα, also known as NR1D1, nuclear receptor subfamily 1, group D, member 1; Rorα, RAR-related orphan receptor alpha; Pparγ, peroxisome proliferator activated receptor gamma) were significantly changed in diabetes [33–36]. Although the master circadian system is located in the suprachiasmatic nucleus of the anterior hypothalamus, peripheral organs are also involved, including heart [37], liver [34], kidney, lung, and pancreas [35], indicating that dysfunction of circadian rhythms may be an underlying mechanism for DKD. Studies have investigated the circadian rhythms with DKD, but most of them mainly focused on blood pressure circadian rhythm; blood pressure circadian rhythm of CKD patients frequently shows a non-dipper pattern. The average 24-h, daytime, and

This work is licensed under Creative Common Attribution-NonCommercial-NoDerivatives 4.0 International (CC BY-NC-ND 4.0)

Indexed in: [Current Contents/Clinical Medicine] [SCI Expanded] [ISI Alerting System] [ISI Journals Master List] [Index Medicus/MEDLINE] [EMBASE/Excerpta Medica] [Chemical Abstracts/CAS]

Table 5. Small molecule drugs predicted by Cmap database.

Cmap name	Mean	N	Enrichment	P	Percent non-null
Thioguanosine	0.729	4	0.927	0.00004	100
Withaferin A	0.727	4	0.826	0.00145	100
DL-thiorphan	0.71	2	0.942	0.0065	100
5230742	0.675	2	0.941	0.00654	100
Menadione	0.664	2	0.935	0.00797	100
Roxithromycin	0.651	4	0.846	0.0008	100
Clomipramine	0.65	4	0.801	0.00298	100
Prestwick-559	0.62	3	0.775	0.02285	100
Repaglinide	0.604	4	0.791	0.00372	100
Daunorubicin	0.575	4	0.76	0.00627	100
Quinostatin	0.569	2	0.858	0.04094	100
Procyclidine	0.558	4	0.702	0.01637	75
Hydrastine Hydrochloride	0.547	4	0.754	0.00702	100
Liothyronine	0.536	4	0.655	0.03268	75
Fluspirilene	0.533	4	0.719	0.01253	100
(+)-Isoprenaline	0.526	4	0.762	0.00605	100
Zimeldine	0.518	5	0.759	0.00194	100
Flunisolide	0.506	6	0.608	0.01128	83
MG-262	0.504	3	0.754	0.02944	100
Meclozine	0.495	5	0.667	0.01077	80
Abamectin	0.489	4	0.716	0.01325	75
Buflomedil	0.487	4	0.704	0.01593	75
Cetirizine	0.484	4	0.707	0.01528	75
15-delta prostaglandin J2	0.481	15	0.531	0.00024	80
beta-escin	0.479	6	0.649	0.00544	83
Sulfamethoxazole	0.474	5	0.57	0.04652	80
Thiostrepton	0.473	4	0.632	0.04579	75
STOCK1N-35215	0.461	3	0.711	0.04729	66
PNU-0251126	0.456	6	0.599	0.01327	83
Resveratrol	0.452	9	0.497	0.01369	77
Bufexamac	0.431	4	0.668	0.02682	75
Furaltadone	0.427	6	0.564	0.02543	66
Verteporfin	0.424	3	0.711	0.04719	66
Tanespimycin	0.414	62	0.432	0	69
Pempidine	0.413	5	0.632	0.01922	60

This work is licensed under Creative Common Attribution-NonCommercial-NoDerivatives 4.0 International (CC BY-NC-ND 4.0)

Indexed in: [Current Contents/Clinical Medicine] [SCI Expanded] [ISI Alerting System] [ISI Journals Master List] [Index Medicus/MEDLINE] [EMBASE/Excerpta Medica] [Chemical Abstracts/CAS]

Table 5 continued. Small molecule drugs predicted by Cmap database.

Cmap name	Mean	N	Enrichment	P	Percent non-null
Clotrimazole	0.405	5	0.583	0.03893	60
Carteolol	–0.41	4	–0.704	0.01585	75
Iohexol	–0.422	4	–0.693	0.0188	75
Rotenone	–0.422	4	–0.64	0.04008	75
Isoflupredone	–0.426	3	–0.796	0.01723	66
Cefaclor	–0.435	4	–0.661	0.02988	75
Timolol	–0.444	4	–0.651	0.03515	75
ethionamide	–0.446	3	–0.74	0.03603	66
3-acetamidocoumarin	–0.447	4	–0.755	0.00734	75
alpha-yohimbine	–0.447	3	–0.73	0.04044	66
Cefotiam	–0.456	4	–0.773	0.00539	75
Erythromycin	–0.457	5	–0.667	0.00955	80
Felbinac	–0.472	4	–0.81	0.00253	75
Streptozocin	–0.472	4	–0.806	0.00277	75
Terazosin	–0.483	4	–0.685	0.02158	75
Fursultiamine	–0.508	4	–0.637	0.04187	75
Benzathine benzylpenicillin	–0.524	4	–0.639	0.04048	75
Ambroxol	–0.551	4	–0.687	0.02077	75
Clorsulon	–0.618	4	–0.829	0.00161	100
Cefoperazone	–0.622	3	–0.906	0.00162	100
Sulmazole	–0.633	3	–0.893	0.00234	100
Vinblastine	–0.73	3	–0.937	0.00038	100

Mean – the arithmetic mean of the connectivity scores for corresponding instances; N – the number of instances; Enrichment – A measure of the enrichment of those instances in the order list of all instances; P – an estimate of the likelihood that the enrichment of a set of instances in the list of all instances in a given result would be observed by chance.

nighttime blood pressure in the patients with DKD were all significantly higher than those of patients with non-DKD, and these blood pressure parameters were found to be significantly correlated with albuminuria [38,39]. No studies explored the circadian rhythm-related genes in renal tissues of DKD. The present study is the first to show that Arntl is significantly downregulated in the renal tissues of diabetic mice. Arntl encodes a basic helix-loop-helix/Per-Arnt-Sim transcription factor that forms a heterodimer with CLOCK and then binds E-box enhancer elements upstream to activate transcription of Period (Per1, Per2, and Per3) and Cryptochrome (Cry1 and Cry2) genes. Downregulation of Arntl leads to lower expressions of Period and Cryptochrome genes, followed by upregulating cellular proliferation and transformation related genes (Cdkn1a, cyclin-dependent kinase inhibitor 1A; Cyclin E1; Claudin 1 and 12; and sFRP1, and secreted frizzled-related protein 1), contributing to the lesion damages in the kidney [40]. Therefore, restoring normal circadian rhythm by altering the expressions of these genes may be a potential approach for treatment of diabetes and its subsequent DKD [41]. As anticipated, Arntl was significantly upregulated in diabetic mice after TSF treatment, suggesting TSF may exert therapeutical effects on DKD by restoring normal circadian rhythm.

In addition to genes, increasing evidence suggests miRNAs may also be important for the development of DKD by either degrading the target mRNAs or inhibiting their translation via binding to the 3'-untranslated regions (UTR). For example,

This work is licensed under Creative Common Attribution-NonCommercial-NoDerivatives 4.0 International (CC BY-NC-ND 4.0)

Indexed in: [Current Contents/Clinical Medicine] [SCI Expanded] [ISI Alerting System] [ISI Journals Master List] [Index Medicus/MEDLINE] [EMBASE/Excerpta Medica] [Chemical Abstracts/CAS]

miR-21 was demonstrated to promote renal fibrosis in DKD by targeting SMAD7, followed by enhancing TGF-β1-induced epithelial-to-mesenchymal transition [42,43]; downregulated miR-451 leads to overexpression of large multifunctional protease 7 (LMP7), which promotes NF-κB-mediated inflammation in mesangial cells and progression of DKD [44]. Thus, inhibition of miRNAs may be an underlying mechanism for treatment of DKD, which has also been reported by several studies [45,46]. Accordingly, miRNAs that regulated our crucial genes were also predicted and compared with the differentially-expressed miRNAs. The results suggest that only the Arntl-related mmu-miR-669j was significantly differentially expressed in the 2 groups and it has not been reported previously in DKD, indicating mmu-miR-669j may be a new target we identified and needs further experiments to confirm.

Moreover, the small-molecule drugs were also investigated to explore a combined strategy or indirectly demonstrate the role of TSF for treatment of DKD. The results showed withaferin A, DL-thiorphan, and menadione may have potential similar to TSF for treatment of DKD. The treatment effects of some small-molecule drugs on diabetes have also been demonstrated in previous studies. For example, it was reported that withaferin-A treatment marginally reduced the body weight of ob/ob and db/db mice and improved glucose homeostasis, which was also Stat3-mediated [47].

Conclusions

Our study reveals that TSF may be an effective and safe alternative for treatment of DKD via inhibiting Racgap1-stata5-mediated cell proliferation and restoring miR-669j-Arntl-related circadian rhythm. Further *in vitro* and *in vivo* studies are needed to confirm these conclusions, which may be our team's future research focus.

Conflict of interest

None.

References:

1. Whiting DR, Guariguata L, Weil C, Shaw J: IDF diabetes atlas: Global estimates of the prevalence of diabetes for 2011 and 2030. Diabetes Res Clin Pract, 2011; 94: 311–21
2. Parving HH, Lewis JB, Ravid M et al: Prevalence and risk factors for microalbuminuria in a referred cohort of type II diabetic patients: A global perspective. Kidney Int, 2006; 69: 2057–63
3. Packham DK, Alves TP, Dwyer JP et al: Relative incidence of ESRD versus cardiovascular mortality in proteinuric type 2 diabetes and nephropathy: Results from the DIAMETRIC (Diabetes Mellitus Treatment for Renal Insufficiency Consortium) database. Am J Kidney Dis, 2012; 59: 75–83
4. Fried LF, Emanuele N, Zhang JH et al: Combined angiotensin inhibition for the treatment of diabetic nephropathy. N Engl J Med, 2013; 369: 1892–903
5. Akh L: Diabetic nephropathy – complications and treatment. Int J Nephrol Renovasc Dis, 2014; 7: 361–81
6. Fineberg D, Jandeleitdahm KAM, Cooper ME: Diabetic nephropathy: Diagnosis and treatment. Nat Rev Endocrinol, 2013; 9: 713–23
7. Ren F, Tang L, Cai Y et al: Meta-analysis: The efficacy and safety of combined treatment with ARB and ACEI on diabetic nephropathy. Ren Fail, 2015; 37: 548–61
8. Li R, Xing J, Mu X et al: Sulodexide therapy for the treatment of diabetic nephropathy, a meta-analysis and literature review. Drug Des Devel Ther, 2015; 9: 6275–83
9. Efferth T, Li PC, Konkimalla VS, Kaina B: From traditional Chinese medicine to rational cancer therapy. Trends Mol Med, 2007; 13: 353–61
10. Liu JY, Chen XX, Tang CW et al: Edible plants from traditional Chinese medicine is a promising alternative for the management of diabetic nephropathy. J Funct Foods, 2015; 14: 12–22
11. Xiao Y, Liu Y, Yu K et al: The effect of chinese herbal medicine on albuminuria levels in patients with diabetic nephropathy: A systematic review and meta-analysis. Evid Based Complement Alternat Med, 2013; 2013: 937549
12. Li P, Chen Y, Liu J et al: Efficacy and safety of tangshen formula on patients with type 2 diabetic kidney disease: A multicenter double-blinded randomized placebo-controlled trial. PLoS One, 2015; 10: e0126027
13. Zhao H, Xin L, Zhao T et al: Tangshen formula attenuates diabetic renal injuries by upregulating autophagy via inhibition of PLZF expression. PLoS One, 2017; 12: e0171475
14. Zhao T, Sun S, Zhang H et al: Therapeutic effects of tangshen formula on diabetic nephropathy in rats. PLoS One, 2016; 11: e0147693
15. Hu J, Fan X, Meng X et al: Evidence for the involvement of JAK/STAT/SOCS pathway in the mechanism of Tangshen formula-treated diabetic nephropathy. Planta Med, 2014; 80: 614–21
16. Irizarry RA, Hobbs B, Collin F et al: Exploration, normalization, and summaries of high density oligonucleotide array probe level data. Biostatistics, 2003; 4: 249–64
17. Ritchie ME, Phipson B, Wu D et al: limma powers differential expression analyses for RNA-sequencing and microarray studies. Nucleic Acids Res, 2015; 43: e47
18. Szklarczyk D, Franceschini A, Wyder S et al: STRING v10: Protein-protein interaction networks, integrated over the tree of life. Nucleic Acids Res, 2015; 43: D447–52
19. Kohl M, Wiese S, Warscheid B: Cytoscape: Software for visualization and analysis of biological networks. Methods Mol Biol, 2011; 696: 291–303
20. Bader GD, Hogue CW: An automated method for finding molecular complexes in large protein interaction networks. BMC Bioinformatics, 2003; 4: 2
21. Dweep H, Gretz N: miRWalk2. 0: A comprehensive atlas of microRNA-target interactions. Nat Methods, 2015; 12: 697
22. Kang JH, Chae YM, Park KK et al: Suppression of mesangial cell proliferation and extracellular matrix production in streptozotocin-induced diabetic rats by Sp1 decoy oligodeoxynucleotide *in vitro* and *in vivo*. J Cell Biochem, 2008; 103: 663–74
23. Xu F, Wang Y, Cui W et al: Resveratrol prevention of diabetic nephropathy is associated with the suppression of renal inflammation and mesangial cell proliferation: Possible roles of Akt/NF-κB Pathway. Int J Endocrinol, 2016; 2014: 289327
24. Huang X, Su YX, Deng HC et al: Suppression of mesangial cell proliferation and extracellular matrix production in streptozotocin-induced diabetic mice by adiponectin *in vitro* and *in vivo*. Horm Metab Res, 2014; 46: 736–43
25. Corpet A, De KL, Toedling J et al: Asf1b, the necessary Asf1 isoform for proliferation, is predictive of outcome in breast cancer. EMBO J, 2011; 30: 480–93
26. Paul PK, Rabaglia ME, Wang CY et al: Histone chaperone ASF1B promotes human β-cell proliferation via recruitment of histone H3.3. Cell Cycle, 2016; 15: 3191–202
27. Wang Z, Chen J, Zhong MZ et al: Overexpression of ANLN contributed to poor prognosis of anthracycline-based chemotherapy in breast cancer patients. Cancer Chemother Pharmacol, 2017; 79: 535–43

This work is licensed under Creative Common Attribution-NonCommercial-NoDerivatives 4.0 International (CC BY-NC-ND 4.0)

Indexed in: [Current Contents/Clinical Medicine] [SCI Expanded] [ISI Alerting System] [ISI Journals Master List] [Index Medicus/MEDLINE] [EMBASE/Excerpta Medica] [Chemical Abstracts/CAS]

28. Zeng S, Yu X, Ma C et al: Transcriptome sequencing identifies ANLN as a promising prognostic biomarker in bladder urothelial carcinoma. Sci Rep, 2017; 7: 3151
29. Zhou W, Wang Z, Shen N et al: Knockdown of ANLN by lentivirus inhibits cell growth and migration in human breast cancer. Mol Cell Biochem, 2015; 398: 11–19
30. Saigusa S, Tanaka K, Mohri Y et al: Clinical significance of RacGAP1 expression at the invasive front of gastric cancer. Gastric Cancer, 2015; 18: 84–92
31. Adrichem AJV, Wennerberg K: MgcRacGAP inhibition stimulates JAK-dependent STAT3 activity. FEBS Lett, 2015; 589: 3859–65
32. Gubin DG, Nelaeva AA, Uzhakova AE et al: Disrupted circadian rhythms of body temperature, heart rate and fasting blood glucose in pre-diabetes and type 2 diabetes mellitus. Chronobiol Int, 2017; 31: 1–13
33. Lebailly B, Boitard C, Rogner UC: Circadian rhythm-related genes: Implication in autoimmunity and type 1 diabetes. Diabetes Obes Metab, 2015; 17(Suppl. 1): 134–38
34. Ando H, Ushijima K, Yanagihara H et al: Clock gene expression in the liver and adipose tissues of non-obese type 2 diabetic Goto-Kakizaki rats. Clin Exp Hypertens, 2009; 31: 201–7
35. Bostwick J, Nguyen D, Cornélissen G et al: Effects of acute and chronic STZ-induced diabetes on clock gene expression and feeding in the gastrointestinal tract. Mol Cell Biochem, 2010; 338: 203–13
36. Motosugi Y, Ando H, Ushijima K et al: Tissue-dependent alterations of the clock gene expression rhythms in leptin-resistant zucker diabetic fatty rats. Chronobiol Int, 2011; 28: 968–72
37. Young ME, Wilson CR, Razeghi P et al: Alterations of the circadian clock in the heart by streptozotocin-induced diabetes. J Mol Cell Cardiol, 2002; 34: 223–31
38. Li J, Wang F, Jian G et al: Analysis of 24-hour ambulatory blood pressure monitoring in patients with diabetic nephropathy: A hospital-based study. Clin Nephrol, 2013; 79: 199–205
39. Hansen HP, Rossing P, Tarnow L et al: Circadian rhythm of arterial blood pressure and albuminuria in diabetic nephropathy. Kidney Int, 1996; 50: 579–85
40. Gumz, Michelle L, Cheng et al: Regulation of cellular transformation genes by the circadian clock protein Per1 in the kidney. FASEB J, 2011; 25: lb113
41. Wang K, Sun Y, Lin P et al: Liraglutide activates AMPK signaling and partially restores normal circadian rhythm and insulin secretion in pancreatic islets in diabetic mice. Biol Pharm Bull, 2015; 38: 1142–49
42. Mcclelland AD, Herman-Edelstein M, Komers R et al: miR-21 promotes renal fibrosis in diabetic nephropathy by targeting PTEN and SMAD7. Clin Sci, 2015; 129: 1237–49
43. Wang JY, Gao YB, Zhang N et al: miR-21 overexpression enhances TGF-β1-induced epithelial-to-mesenchymal transition by target smad7 and aggravates renal damage in diabetic nephropathy. Mol Cell Endocrinol, 2014; 392: 163–72
44. Sun Y, Peng R, Peng H et al: miR-451 suppresses the NF-kappaB-mediated proinflammatory molecules expression through inhibiting LMP7 in diabetic nephropathy. Mol Cell Endocrinol, 2016; 433: 75–86
45. Wang JY, Gao YB, Zhang N et al: Tongxinluo ameliorates renal structure and function by regulating miR-21-induced epithelial-to-mesenchymal transition in diabetic nephropathy. Am J Physiol Renal Physiol, 2014; 306: 486–95
46. Zhang L, He S, Yang F et al: Hyperoside ameliorates glomerulosclerosis in diabetic nephropathy by downregulating miR-21. Can J Physiol Pharmacol, 2016; 94: 1249–56
47. Lee J, Liu J, Feng X et al: Withaferin A is a leptin sensitizer with strong antidiabetic properties in mice. Nat Med, 2016; 22: 1023–32

This work is licensed under Creative Common Attribution-NonCommercial-NoDerivatives 4.0 International (CC BY-NC-ND 4.0)

Indexed in: [Current Contents/Clinical Medicine] [SCI Expanded] [ISI Alerting System] [ISI Journals Master List] [Index Medicus/MEDLINE] [EMBASE/Excerpta Medica] [Chemical Abstracts/CAS]